Eur. Phys. J. B **53**, 367–374 (2006)
DOI: 10.1140/epjb/e2006-00382-7

THE EUROPEAN PHYSICAL JOURNAL B

Analysis of stability and density waves of traffic flow model in an ITS environment

Z.-P. Li[a] and Y.-C. Liu

Institute of Image Processing and Pattern Recognition, Shanghai Jiao Tong University, 200240 Shanghai, P.R. China

Received 3 August 2006
Published online 18 October 2006 –

Abstract. By introducing relative velocities of arbitrary number of cars ahead into the full velocity difference models (FVDM), we present a forward looking relative velocity model (FLRVM) of cooperative driving control system. To our knowledge, the model is an improvement over the similar extension in the forward looking optimal velocity models (FLOVM), because it is more reasonable and realistic in implement of incorporating intelligent transportation system in traffic. Then the stability criterion is investigated by the linear stability analysis with finding that new consideration theoretically lead to the improvement of the stability of traffic flow, and the validity of our theoretical analysis is confirmed by direct simulations. In addition, nonlinear analysis of the model shows that the three waves: triangular shock wave, soliton wave and kink-antikink wave appear respectively in stable, metastable and unstable regions. These correspond to the solutions of the Burgers equation, Korteweg-de Vries (KdV) equation and modified Korteweg-de Vries (mKdV) equation.

PACS. 89.40.-a Transportation – 64.60.Cn Order-disorder transformations; statistical mechanics of modelsystems – 02.60.Cb Numerical simulation; solution of equations – 05.70.Fh Phase transitions: general studies

1 Introduction

Over the past decades, traffic flow problems have attracted considerable attention in the field of physics [1–6], especially traffic congestion. To explain this phenomenon, a lot of studies in the mathematical models have been done in describing the dynamics of discrete groups of road cars [7–11]. As one of such traffic models, the optimal velocity model (OVM), which is proposed by Bando et al. in 1995 [8], has successfully described the dynamical formation of traffic congestion. In this model, each car is described by a simple differential equation using the optimal velocity function, which is determined on the headway (the distance between the car position and the position of the preceding car). Under a certain condition, OVM successfully provides appearance of spontaneous transitions from freely moving traffic to congested traffic, which has been clarified by linear stability analysis. Moreover, perturbation methods had been adapted to analyze the traffic wave of the OVM by Komatsu and Sasa [12]. They have applied a modified Korteweg-de Vries (mKdV) equation to a traffic jam which is described by a kink-antikink density wave.

Although the OVM is shown to have a universal structure in describing many properties of traffic flow, many improvements have been done to make it fit real traffic behavior. A calibration of the OVM with respect to the empirical data shows that high acceleration and unrealistic deceleration occur in the OVM, and Helbing and Tilch [13] developed a generalized force model (GFM) with a velocity difference term added into the OVM. The simulation results show that the GFM is in good agreement with the empirical data. In 2001 Jiang et al. found out that the GFM exhibited poor delay time of car motion and kinematic wave speed at jam density and proposed a full velocity difference model (FVDM) [14]. In this model both positive and negative velocity difference are taken into account, and the numerical investigations showed that FVDM could described the phase transition of traffic flow and estimate the evolution of traffic congestion.

From the viewpoint of economic value, the most important problem is to maximize the throughput of cars on highways and prevent the traffic congestion. Based on the fact that real-time reporting systems of vehicular information are now becoming widely available, in order to aid emergency dispatch assistance and traffic control management as being an important part of intelligent transportation systems (ITS), the study has been focused on using the information of many other cars to suppress the appearance of traffic congestion efficiently. In 2003 and 2004, Hasebe et al. [15,16] suggested a "forward looking" optimal velocity model (FLOVM) applied to such

[a] e-mail: lizhipeng0827@sjtu.edu.cn

a cooperative driving control system and Ge et al. [17] investigated dynamic behavior near the critical point of the model. In their models, the optimal function is extended to incorporate the effect from many cars in front by introducing into the headway of arbitrary number of cars ahead. They had verified that a certain set of parameters exist in their models make traffic flow "most stable".

However, there essentially exist some disadvantages in performing such a cooperative driving control system run by FLOVM in ITS environment. First of all, the precondition of applying FLOVM to decide the traffic behavior is that the position of all cars should be obtained accurately. At present positioning services for civil users are mostly provided by GPS, which is a satellite navigation system funded and controlled by the US Department of Defense (DOD). Unfortunately, the GPS data of the receiver have some errors, which consist of noise, bias, and blunders. Although we can improve the accuracy of the GPS signal regardless of the extra fee of cost, the accumulative errors of positions of many cars ahead in FLOVM will also lead to failure of our endeavor. Secondly, there are always many cars entering or leaving from any location of road network at any time in real traffic, it will lead to some separations between successive cars varying abruptly. Such situation will consumedly increase the possibility that driver conducts error operation for reacting to the error information of others, and even further leads to a sudden collision, which extensively decrease the feasibility of suppressing traffic congestion for our purpose by incorporating the ITS application.

But, do there exist other regulations for incorporating the information of many cars ahead? And can other form of extended model get rid of all above defects exist in the FLOVM? Here we shall concentrate our attention on such direction. As we know, the instantaneous velocity of each car can accurately obtained by velocity indicator in car based on ITS application environment. It is very realistic and prospective that the stability of the traffic flow can be enhanced further by use of such a data. In this paper, we try to present a differential-difference equation of traffic dynamics which extends the FVDM to take into account the relative velocities of arbitrary number of ones ahead. Since our model incorporates not only the relative velocity of the considered car but also the relative velocities of many cars ahead of considered one, we call it forward looking relative velocity model (FLRVM), which will be proved to overcome the difficult cases described above. Moreover, linear stability analysis shows that the model is stabilized by taking into account the relative velocities of many cars ahead. We will compare the analytical result with that from the numerical simulation. From the nonlinear analysis, it is shown that three different traffic waves appear in stable, unstable and metastable regions.

This paper is organized as follows: the previous car-following models, including the OVM, the FVDM and the FLOVM are reviewed in Section 2. In Section 3 and Section 4 we introduce our dynamical equation for traffic flow and the stability criterion of it is investigated in an analytic method respectively. In Section 5 we analyse the density wave for a traffic flow by means of the perturbation methods in the three regions, stable, metastable and unstable regions. The stability condition of traffic flow is investigated by means of simulation; we shall see that the proposed model works very well for our purpose by conducting direction simulations in Section 6. Finally, conclusions are summarized.

2 Previous car-following models

2.1 The optimal velocity model

In 1995, Bando et al. [8] have analyzed a traffic model called the optimal velocity model (OVM), In the OVM, the acceleration of the jth vehicle at time t is determined by the difference between the actual velocity $v_j(t)$, and an optimal velocity $V(\Delta x_j(t))$, which depends on the headway $\Delta x_j(t)$ to the car in the front:

$$\frac{dv_j(t)}{dt} = a[V(\Delta x_j(t)) - v_j(t)] \tag{1}$$

where a is the sensitivity of a driver and is given by inverse of the delay time. The comparison with field data suggests that the OVM encountered the problems of high acceleration and unrealistic deceleration.

2.2 The full velocity difference model

By taking the velocity difference into account, Jiang et al. [14] developed a full velocity difference model (FVDM) based on the OVM. The traffic model described by the following equation of motion of car j:

$$\begin{aligned} \frac{dv_j(t)}{dt} &= a\left[V(\Delta x_j(t)) - v_j(t)\right] + k\Delta v_j(t) \\ \Delta v_{j+l}(t) &= v_{j+l+1} - v_{j+l} \end{aligned} \tag{2}$$

where k is a constant. Simulation results show that FVDM does not appear unrealistically high acceleration which occurs in the OVM. Moreover, this model can predicts correct delay time of car motion and kinematic wave speed at jam density.

2.3 Forward looking optimal velocity model

With the fast development of the intelligent traffic system (ITS), drivers can receive information of other cars on roads, and some scholars suggest that it is possible to improve the stability of traffic flow and suppress the appearance of traffic jam in light of the information. In 2003, Hasebe, Nakayama, and Sugiyama presented the forward looking optimal velocity model (FLOVM) [15], which bases the idea that a driver looks at many vehicles ahead of him/her. In 2004, H.X. Ge et al. suggest a

kind of FLOVM [17], which is described by the following differential equation:

$$\frac{dv_j(t)}{dt} = a[V\left(\sum_{l=1}^{n}\alpha_l(\Delta x_{l+j}(t))\right) - v_j(t)] \qquad (3)$$

where α_l is the weighted function of $\Delta x_{l+j}(t)$. From equation (3) we can observe that this model incorporating an ITS by taking into account headways of n-cars ahead. The FLOVM is verified to further stabilize traffic flow than the single car consideration in the OVM. However, it still has some problems in obtaining the accurate headway under the ITS environment.

3 Forward looking relative velocity model

In incorporating multivehicle consideration in real traffic, if we can accurately get the position of each car, the implement of the FLOVM is reasonable and charming; otherwise it will extensively affect our purpose to improve the stability of traffic flow. This is the just reason why we find out another means that applies to a cooperative driving control system. Now, according to the idea mentioned in the Introduction, we extend the FVDM by incorporating the relative velocities of n-cars ahead, and then get a new model, the forward looking relative velocity model. The dynamical model of traffic is presented as follows,

$$\frac{dx_j(t+\tau)}{dt} = V(\Delta x_j(t), \sum_{l=0}^{n}\alpha_l \Delta v_{j+l}(t))$$
$$\alpha_l = \left(\frac{1}{5}\right)^{(l+1)} \qquad (4)$$

where α_l is the weighted function of $\Delta v_{j+l}(t)$, and $V(\Delta x_j(t)\ , \sum_{l=0}^{n}\alpha_l \Delta v_{j+l}(t))$ is the extended OV function including variables of the headway and relative velocities. The idea of the model is that a driver adjusts the car velocity at time t according to the observed headway, and the relative velocities of n cars ahead at time $t-\tau$ to reach the optimal velocity, where τ is the delay time which is the time lag before reaching the optimal velocity.

Assuming that the delay time τ is small, Taylor expansion both sides of equation (4) leads to,

$$\frac{dv_j(t)}{dt} = a\left[V(\Delta x_j(t)) - \frac{dx_j(t)}{dt}\right] + k\sum_{l=0}^{n}\alpha_l \Delta v_{j+l}(t) \quad (5)$$

where we assume that the extended OV is $V(\Delta x_j(t), \sum_{l=0}^{n}\alpha_l \Delta v_{j+l}(t)) = V(\Delta x_j(t)) + \lambda\sum_{l=0}^{n}\alpha_l \Delta v_{j+l}(t)$, a is the sensitivity of a driver to the observed headway $\Delta x_j(t)$, $a = \frac{1}{\tau}$; k is the sensitivity of response to the stimulus $\sum_{l=0}^{n}\alpha_l \Delta v_{j+l}(t)$ and is taken to be $k = \frac{\lambda}{\tau}$. It is assumed that λ is a constant independent of time, velocity and position, which is called the response factor to the sum of relative velocities.

Generally, the optimal velocity function $V(x)$ is a monotonically increasing function and it has an upper bound [18]. According to the original OVM, we will take a hyperbolic tangent function as

$$V(\Delta x_j(t)) = \tanh(\Delta x_j(t) - h_c) + \tanh(h_c) \qquad (6)$$

where $h_c = 4.0$ which gives the safe distance. In order to deal with a more realistic traffic model, we can conduct a calibration of all parameters of the model, but we will not consider this here because we are interested in the characteristic properties of our model.

It is convenient to rewrite equation (4) by using the asymmetric forward difference, which is reformulated,

$$x_j(t+2\tau) - x_j(t+\tau) = V(\Delta x_j)\tau + \lambda\left\{\sum_{l=0}^{n}\alpha_l[\Delta x_{j+l}(t+\tau) - \Delta x_{j+l}(t)]\right\}. \quad (7)$$

Now, we discuss the expression in the right side of equation (5). Comparing with the FLOVM, FLRVM differs in the interaction term, where FLOVM extends the original OVM with other car's headway with some errors, while FLRVM suggests extending car interaction by other car's relative velocity, which is equal to the instantaneous velocity difference of the successive velocity. From this point of view, FLRVM incorporates the ITS application more exactly, which verifies that the new consideration in our model is reasonable and realistic.

4 Linear stability analysis

Next we explore whether the proposed model can further stabilize traffic flow similar to the FLOVM. We apply the linear stability method to the extended model described by equation (7). We consider the stability of uniform traffic flow, which can be defined by such a state that all cars move with the identical headway h and the optimal velocity $V(h)$, and it can be written as,

$$x_j^{(0)}(t) = V(b)t + jh, \quad b = L/N \qquad (8)$$

where $N$is the total number of cars. When Ge et al. discussed their model, a restriction condition that the sum of all the weighted function of headway introduced is equal to 1 was imposed on the FLOVM in order to satisfy above solution of steady state [17]. It consumedly constricts the selection of the weighted function applied to the FLOVM. But here we can observe that it is apparent that the following solution of steady state flow satisfies the dynamical equation (7) with any form of the weighted function α_l. From this point, the FLRVM holds much more flexibility than the FLOVM.

To see whether the solution (8) is stable or not, we add a small disturbance $y_j(t)$,

$$x_j(t) = x_j^{(0)}(t) + y_j(t). \qquad (9)$$

Then the linearized equation is obtained

$$y_j(t+2\tau) = y_j(t+\tau) + V'(h)\tau\Delta y_j + \lambda\left\{\sum_{l=0}^{n}\alpha_l[\Delta y_{j+l}(t+\tau) - \Delta y_{j+l}(t)]\right\}. \quad (10)$$

By expanding $y_j(t) = e^{ikj+zt}$, the following equation of z is obtained

$$(e^{z\tau}-1)[e^{z\tau} - \lambda\sum_{l=0}^{n}\alpha_l(e^{ik}-1)] = V'(h)\tau(e^{ik}-1). \quad (11)$$

The solution of equation (11) is:

$$z = z_1(ik) + z_2(ik)^2 + ... \quad (12)$$

The first- and second-order terms of ik are obtained,

$$z_1 = V'(h),$$
$$z_2 = \frac{V'(h)}{2} - \frac{3[V'(h)]^2}{2} + \lambda V'(h)\sum_{l=0}^{n}\alpha_l. \quad (13)$$

If z_2 is a negative value, the uniformly steady-state flow becomes unstable for long-wavelength modes, while the uniform flow is stable when z_2 is a positive value. Thus the neutral stability criteria for this steady state are summarized as follows:

$$V'(h) < \frac{1+2\lambda\sum_{l=0}^{n}\alpha_l}{3\tau}. \quad (14)$$

Comparing the result with that of the original OVM [19], we can conclude that the FLRVM is stabilized in the region

$$\frac{1}{3\tau} < V'(h) < \frac{1+2\lambda\sum_{l=0}^{n}\alpha_l}{3\tau}$$

by the effect of velocity interactions of many cars ahead, which means that by introducing the relative velocity of many cars ahead into the original car-following model, the traffic flow becomes more stable similar to that by taking into account the headway of many cars ahead. It can also be obtained that the more we consider the effects of the relative velocities of cars ahead, the more stable the traffic flow will be.

5 Nonlinear stability analysis

Vehicle density could fluctuate for various reasons to form a density wave in traffic flow, which leads to the traffic jams. Different nonlinear wave equations have been derived to describe the corresponding density waves from a great number of earlier models of car-following. In order to examine this respect of our model, here we will investigate the nonlinear dynamics of traffic jams. We will consider the slowly varying behavior in the stable, the metastable and the unstable region with the help of a small positive scaling parameter ε.

In order to extract slow scales for the space variable $j$and the time variable t [20,21], here we define the slow variables X and T for $0 < \varepsilon \leq 1$ as follows,

$$X = \varepsilon^p(j+bt), \quad T = \varepsilon^q t \quad (15)$$

where b is a constant to be determined. Let

$$\Delta x_j(t) = h + \varepsilon^m R(X,T). \quad (16)$$

In the expressions of equations (15, 16), m, p and q are parameters which will be determined for following discussion in the stable region [22], near the neutral stability line [12] and in the unstable region [23].

We rewrite equation (7) as

$$\Delta x_j(t+2\tau) - \Delta x_j(t+\tau) = [V(\Delta x_{j+1}) - V(\Delta x_j)]\tau + \lambda\left\{\sum_{l=0}^{n}\alpha_l[\Delta x_{j+l+1}(t+\tau) - \Delta x_{j+l+1}(t) - \Delta x_{j+l}(t+\tau) + \Delta x_{j+l}(t)]\right\}. \quad (17)$$

Substituting equations (15) and (16) into equation (17) and making the Taylor expansions to the fifth order of ε, we can obtain the following nonlinear partial differential equation

$$\begin{aligned}
&\varepsilon^{p+m}b\tau\partial_X R + \varepsilon^{q+m}\tau\partial_T R + \varepsilon^{2p+m}\frac{3b^2\tau^2}{2}\partial_X^2 R \\
&+ \varepsilon^{2q+m}\frac{3\tau^2}{2}\partial_T^2 R + \varepsilon^{p+q+m}3b\tau^2\partial_T\partial_X R \\
&+ \varepsilon^{3p+m}\frac{7b^3\tau^3}{6}\partial_X^3 R + \varepsilon^{2p+q+m}\frac{7b^2\tau^3}{2}\partial_T\partial_X^2 R \\
&+ \varepsilon^{4p+m}\frac{15b^4\tau^4}{24}\partial_X^4 R = \Bigg[\varepsilon^{p+m}V'(h)\partial_X R \\
&+ \varepsilon^{2p+m}\frac{V'(h)}{2}\partial_X^2 R + \varepsilon^{3p+m}\frac{V'(h)}{6}\partial_X^3 R \\
&+ \varepsilon^{4p+m}\frac{V'(h)}{24}\partial_X^4 R + \varepsilon^{p+2m}\frac{V''(h)}{2}\partial_X R^2 \\
&+ \varepsilon^{2p+2m}\frac{V''(h)}{4}\partial_X^2 R^2 + \varepsilon^{3p+2m}\frac{V''(h)}{24}\partial_X^3 R^2 \\
&+ \varepsilon^{p+3m}\frac{V'''(h)}{6}\partial_X R^3 + \varepsilon^{2p+3m}\frac{V'''(h)}{12}\partial_X^2 R^3 \\
&+ \varepsilon^{3p+3m}\frac{V'''(h)}{36}\partial_X^3 R^3\Bigg]\tau + \lambda\sum_{l=0}^{n}\alpha_l\Bigg[\varepsilon^{2p+m}b\tau\partial_X^2 R \\
&+ \varepsilon^{p+q+m}\tau\partial_T\partial_X R + \varepsilon^{3p+m}\frac{3b\tau(b\tau+2l+1)}{6}\partial_X^3 R \\
&+ \varepsilon^{4p+m}\frac{4(b\tau)^3 + 6(b\tau)^2(2l+1) + 4b\tau(3l^2+3l+1)}{24}\partial_X^4 R\Bigg]
\end{aligned} \quad (18)$$

where $\partial_T = \frac{\partial}{\partial T}$, $\partial_X = \frac{\partial}{\partial X}$, $\partial_X\partial_T = \frac{\partial^2}{\partial X\partial T}$, $V'(\Delta x) = \frac{dV(\Delta x)}{d\Delta x}\Big|_{\Delta x=h}$, and $V'(\Delta x) = \frac{dV^3(\Delta x)}{d\Delta x^3}\Big|_{\Delta x=h}$.

5.1 Stable flow region

In the stable traffic flow the long-wave models is considered by taking $p = 1$, $q = 2$, and $m = 1$. Substituting the values of these parameters into equation (18), one obtains the following partial differential equation:

$$\varepsilon^2[b-V'(h)]\partial_X R+\varepsilon^3\left[\partial_T R+\left\{\frac{3V'^2(h)\tau}{2}-\frac{\left(1+2\lambda\sum_{l=0}^{n}\alpha_l\right)V'(h)}{2}\right\}\partial_X^2 R-V''(h)R\partial_X R\right]=0. \tag{19}$$

By taking $b = V'(h)$, the second order of ε is eliminated from equation (19), which is

$$\partial_T R-V''(h)R\partial_X R=\left[\frac{\left(1+2\lambda\sum_{l=0}^{n}\alpha_l\right)}{2}-\frac{3V'(h)\tau}{2}\right]V'(h)\partial_X^2 R. \tag{20}$$

In accordance with criterion (14), the coefficients $[(1 + 2\lambda\sum_{l=0}^{n}\alpha_l)/2 - 3V'(h)\tau/2]$ of the second derivatives are positive values in the stable traffic region. Thus, in the stable region, equation (20) is just the Burgers equation, of which the solution is a train of N-shock waves and is given by

$$R(X,T)=\frac{1}{|V''(h)|\,T}\left[X-\frac{1}{2}(\eta_j+\eta_{j+1})\right]-\frac{1}{2\,|V''(h)|\,T}\times(\eta_{j+1}-\eta_j)\tanh\left[\frac{C_1}{4\,|V''(h)|\,T}(\eta_{j+1}-\eta_j)(X-\xi_j)\right]. \tag{21}$$

Here $C_1 = (1 + 2\lambda\sum_{l=0}^{n}\alpha_l)V'(h)/2 - 3V'^2(h)\tau/2$ and η_j and ξ_j represent the coordinates of the intersection of the slopes with the x axis and the coordinates of the shock fronts respectively. According to equation (21), the triangular shock wave in free flow propagates backward with propagation velocity b. Moreover, we can observe that the $R(X,T) \to 0$ when $t \to \infty$, which means that the any density wave in free traffic flow will evolves to a homogeneous flow in the course of time.

5.2 Unstable flow region

Next we investigate the nonlinear waves near the critical point $h = h_c$, which is a turning point (infection point) with $V''(h_c) = 0$. The turning point will help us to obtain the kink-antikink density wave solution representing the traffic jam.

By taking $p = 1$, $q = 3$ and $m = 1$, one obtains the following nonlinear partial differential equation from equation (18)

$$\begin{aligned}\varepsilon^2[b-V'(h_c)]\partial_X R+\varepsilon^3&\left[\frac{3b^2\tau}{2}\partial_X^2 R-\frac{V'(h_c)}{2}\partial_X^2 R^2-\frac{V''(h_c)}{2}\partial_X R^2-\lambda\sum_{l=0}^{n}\alpha_l b\partial_X^2 R\right]+\varepsilon^4\left[\partial_T R+\frac{7b^3t^2}{6}\partial_X^3 R\right.\\&-\frac{V'(h_c)}{6}\partial_X^3 R-3\lambda\sum_{l=0}^{n}\alpha_l\frac{(1+2l+b\tau)b}{6}\partial_X^3 R\\&\left.-\frac{V''(h_c)}{4}\partial_X^2 R^2+\frac{V'''(h_c)}{6}\partial_X R^3\right]\\&+\varepsilon^5\left[3b\tau\partial_T\partial_X R+\frac{15b^4\tau^3}{24}\partial_X^4 R\right.\\&-\frac{V'(h_c)}{24}\partial_X^4 R-\frac{V''(h_c)}{24}\partial_X^3 R^2-\frac{V'''(h)}{12}\partial_X^2 R^3\\&-\frac{\lambda\sum_{l=0}^{n}\alpha_l[4b^3\tau^2+6b^2\tau(2l+1)+4b(3l^2+3l+1)]}{24}\\&\left.\times\partial_X^4 R\right]=0.\end{aligned} \tag{22}$$

We denote $V' = V'(h)$ and $V''' = V'''(h_c)$. Near the critical point, $\tau = (1+\varepsilon^2)\tau_c$, by taking $b = V'$, and eliminating the second- and third-order terms of ε, we can obtain a simplified equation

$$\varepsilon^4\left[\partial_T R-m_1V'\partial_X^3 R+m_2\partial_X R^3\right]+\varepsilon^5\left[m_3\,\partial_X^2 R+m_4\partial_X^2 R^3\,-m_5\partial_X^4 R\right]=0 \tag{23}$$

where

$$\begin{aligned}m_1&=\frac{9-7\left(1+2\lambda\sum_{l=0}^{n}\alpha_l\right)^2+9\lambda\sum_{l=0}^{n}\alpha_l\left(4+6l+2\lambda\sum_{l=0}^{n}\alpha_l\right)}{54}V',\\ m_2&=-\frac{V'''}{6},\quad m_3=\frac{\left(1+2\lambda\sum_{l=0}^{n}\alpha_l\right)V'}{2},\quad m_4=\frac{V'''}{12}\\ m_5&=\frac{9-5\left(1+2\lambda\sum_{l=0}^{n}\alpha_l\right)^3}{216}+\frac{\lambda}{108}\sum_{l=0}^{n}\alpha_l\left[2\left(1+2\lambda\sum_{l=0}^{n}\alpha_l\right)^2\right.\\&\left.-9(2l+1)\left(1+2\lambda\sum_{l=0}^{n}\alpha_l\right)+18(3l^2+3l+1)\right].\end{aligned} \tag{24}$$

In order to derive the regularized equation, we make the following transformations

$$T'=m_1V'T,\quad R=\sqrt{\frac{m_1}{m_2}}R'. \tag{25}$$

$$\Delta x_j(t) = h_c + \sqrt{-\frac{18 - 14\left(1 + 2\lambda\sum_{l=0}^{n}\alpha_l\right)^2 + 18\lambda\sum_{l=0}^{n}\alpha_l\left(4 + 6l + 2\lambda\sum_{l=0}^{n}\alpha_l\right)}{9V'''} cV'\left(\frac{\tau}{\tau_c} - 1\right)} \tanh\sqrt{\frac{c}{2}\left(\frac{\tau}{\tau_c} - 1\right)} \times \left[j + \left(1 - \frac{9 - 7\left(1 + 2\lambda\sum_{l=0}^{n}\alpha_l\right)^2 + 9\lambda\sum_{l=0}^{n}\alpha_l\left(4 + 6l + 2\lambda\sum_{l=0}^{n}\alpha_l\right)}{27} cV'\left(\frac{\tau}{\tau_c} - 1\right)\right) t\right]. \quad (27)$$

$$c = \frac{135\left(1 + 2\lambda\sum_{l=0}^{n}\alpha_l\right)}{5 - 17\lambda\sum_{l=0}^{n}\alpha_l - 37\left(\lambda\sum_{l=0}^{n}\alpha_l\right)^2 - 12\left(\lambda\sum_{l=0}^{n}\alpha_l\right)^3 + 135\lambda\sum_{l=0}^{n}\alpha_l l + 54\lambda\sum_{l=0}^{n}\alpha_l l^2 - 9\lambda\sum_{l=0}^{n}\alpha_l(2l+1)\left(1 + 2\lambda\sum_{l=0}^{n}\alpha_l\right)}.$$

$$\varepsilon^3[b - V'(h)]\partial_X R + \varepsilon^4\left[\frac{3b^2\tau}{2}\partial_X^2 R - \frac{V'(h)}{2}\partial_X^2 R^2 - \lambda\sum_{l=0}^{n}\alpha_l b\partial_X^2 R\right] + \varepsilon^5\left[\partial_T R + \frac{7b^3t^2}{6}\partial_X^3 R - \frac{V''(h)}{2}\partial_X R^2 - \frac{V'(h)}{6}\partial_X^3 R - 3\lambda\sum_{l=0}^{n}\alpha_l\frac{(1 + 2l + b\tau)b}{6}\partial_X^3 R\right] + \varepsilon^6\left[3b\tau\partial_T\partial_X R + \frac{15b^4\tau^3}{24}\partial_X^4 R - \frac{V''(h)}{4}\partial_X^2 R^2 - \lambda\sum_{l=0}^{n}\alpha_l\partial_T\partial_X R - \frac{\lambda\sum_{l=0}^{n}\alpha_l[4b^3\tau^2 + 6b^2\tau(2l+1) + 4b(3l^2+3l+1)]}{24}\partial_X^4 R\right] = 0. \quad (28)$$

Thus, we obtain the regularized mKdV equation with perturbed term:

$$\partial_{T'}R' - \partial_X^3 R' + \partial_X R'^3 + \varepsilon\sqrt{\frac{1}{m_1}}\left[m_3\partial_X^2 R' + \frac{m_1 m_4}{m_2}\partial_X^2 R'^3 - m_5\partial_X^4 R'\right] = 0. \quad (26)$$

Thus, one obtains the kink-antikink solution of the headway ($V' = 1$, $V''' = -2$) from equation (26):

see equation (27) above

According to the general solution presented by Ge et al. [24], we can obtain the selected value of propagation velocity c for the kink-antikink solution (27) as follows,

see equation above

equation (26) shows that the kink-antikink density wave, which is described by the solution of the mKdV equation, appears near the critical point as the density wave in the unstable region.

5.3 Metastable flow region

Next we consider the case of $p = 1$, $q = 3$ and $m = 2$, which will help us to obtain the following nonlinear partial differential equation near the neutral stability from equation (18).

see equation (28) above

Analogously, we denote $V'(h) = V'$ and $V''(h) = V''$. Near the neutral stability line $\tau_s = (1 + 2\lambda\sum_{l=0}^{n}\alpha_l)/3V'(h)$, $\tau = (1-\varepsilon^2)\tau_s$. Taking $b = V'(h)$ and eliminating the third- and fourth-order terms of ε from equation (28) result in a simplified equation

$$\varepsilon^4\left[\partial_T R - g_1 V'\partial_X^3 R + g_2 R\partial_X R\right] + \varepsilon^5\left[g_3\partial_X^2 R - g_4\partial_X^2 R^2 - g_5\partial_X^4 R\right] = 0 \quad (29)$$

where

$$g_1 = \frac{9 - 7\left(1 + 2\lambda\sum_{l=0}^{n}\alpha_l\right)^2 + 9\lambda\sum_{l=0}^{n}\alpha_l\left(4 + 6l + 2\lambda\sum_{l=0}^{n}\alpha_l\right)}{54}V',$$

$$g_2 = V'', \quad g_3 = \frac{\left(1 + 2\lambda\sum_{l=0}^{n}\alpha_l\right)V'}{2}, \quad g_4 = \frac{V''}{4}$$

$$g_5 = \frac{9 - 5\left(1 + 2\lambda\sum_{l=0}^{n}\alpha_l\right)^3}{216} + \frac{\lambda}{108}\sum_{l=0}^{n}\alpha_l\left[2\left(1 + 2\lambda\sum_{l=0}^{n}\alpha_l\right)^2 - 9(2l+1)\left(1 + 2\lambda\sum_{l=0}^{n}\alpha_l\right) + 18(3l^2 + 3l + 1)\right].$$

$$A=\frac{42+252\lambda\sum_{l=0}^{n}\alpha_l+126\left(\lambda\sum_{l=0}^{n}\alpha_l\right)^2+\left(1134\lambda+2268\lambda^2\sum_{l=0}^{n}\alpha_l\right)\sum_{l=0}^{n}\alpha_l l-420\left(\lambda\sum_{l=0}^{n}\alpha_l\right)^3}{14+161\lambda\sum_{l=0}^{n}\alpha_l+230\left(\lambda\sum_{l=0}^{n}\alpha_l\right)^2+60\left(\lambda\sum_{l=0}^{n}\alpha_l\right)^3+403\lambda\sum_{l=0}^{n}\alpha_l l-240\lambda\sum_{l=0}^{n}\alpha_l l^2-90\lambda\sum_{l=0}^{n}\alpha_l(2l+1)\left(1+2\lambda\sum_{l=0}^{n}\alpha_l\right)}.$$

We conduct the following transformations

$$T=\sqrt{g_1}T',\quad X=-\sqrt{g_1}X',\quad R=\frac{1}{g_2}R'. \tag{30}$$

Thus, we obtain the regularized KdV equation with perturbed term:

$$\partial_{T'}R'-\partial^3_{X'}R'+R'\partial_X R'+\varepsilon\sqrt{\frac{1}{g_1}}\left[-g_3\partial^2_X R'+\frac{g_5}{g_2}\partial^2_X R'^2+\frac{g_4}{g_1}\partial^4_X R'\right]=0. \tag{31}$$

We ignore the $O(\varepsilon)$ term in equation (31), and obtain the soliton solution of headway as the desired solution,

$$\Delta x_j(t)=h+\frac{A}{V''}\left(1-\frac{t}{t_s}\right)\sec h^2\left[\sqrt{\frac{9A}{4\left[1+4\lambda\sum_{l=0}^{n}\alpha_l+27\lambda\sum_{l=0}^{n}\alpha_l l-5\left(\lambda\sum_{l=0}^{n}\alpha_l\right)^2\right]V'}(1-\frac{t}{t_s})}\right]\times\left\{j+\left[V'+\frac{A}{3}\left(1-\frac{t}{t_s}\right)\right]t\right\}. \tag{32}$$

The selected value of amplitude$A$ for the KdV equation is determined from the perturbation terms in equation (31) as follows

see equation above

From above analysis from our model, we can observe that three nonlinear wave equations is derived to describe the corresponding density waves, among which the Burgers equation, KdV equation and mKdV equation depict the density waves appearing in the distinct regions, respectively.

6 Simulation tests

To check the validity of our analysis above, we carry out numerical simulation for our model described by equations (6) and (7) under the periodic boundary condition. The initial headway is chosen as follows:

$$\Delta x_j(0)=\Delta x_j(1)=4.0m,\quad (j\neq 50,51) \tag{33}$$
$$\Delta x_j(0)=\Delta x_j(1)=4.0-0.1,\quad (j=50) \tag{34}$$
$$\Delta x_j(0)=\Delta x_j(1)=4.0+0.1,\quad (j=51) \tag{35}$$

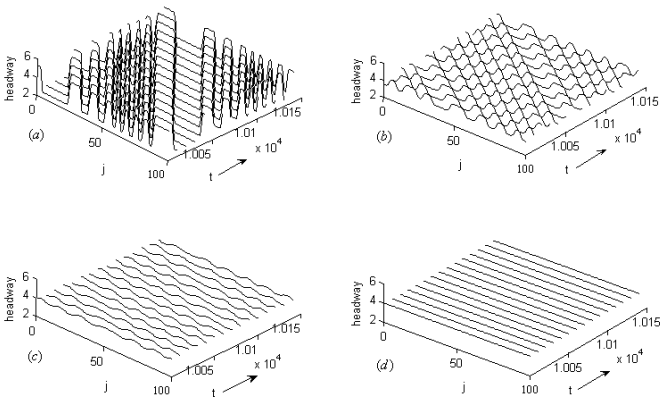

Fig. 1. The spatio-temporal evolution of the headway for (a) $n=0$,(b) $n=1$, (c) $n=2$, and (d) $n=3$ respectively. ($a=2$ and $\lambda=1$).

where the total number of cars is 100. Figure 1 shows the typical traffic patterns after a sufficiently long time $t=10^4$. The spatio-temporal evolution of the headway for various number n of the relative velocities of cars in front has different properties. The patterns (a), (b), (c), and (d) show the time evolutions of the headway profile according to the FLRVM for $n=0,1,2,3$, where $a=2$ and $\lambda=1$. The pattern (a) with $n=0$ and the pattern (b) with $n=1$ correspond to that of the OVM and the FVDM respectively. In the patterns (a), (b), and (c) the phase transit from free flow to jammed traffic is observed and the jams propagate backward as the kink-antikink density wave. Figure 2 shows the headway profile obtained at sufficiently large time $t=10^4$. With increasing number n of the relative velocities of the cars ahead, the amplitude of the density wave is weakened and initial small disturbances decay and initial traffic flow with a non-uniform density profile evolves to a uniformly traffic flow which is shown in pattern (d) if we set $n=3$. Therefore, all the results show that the effect of the relative velocities of the cars ahead can stabilize the traffic flow just as the FLOVM.

7 Summary

By introducing the relative velocities of the cars in front into the FVDM, a forward looking relative velocities model (FLRVM) is proposed to constructing a cooperative driving system for highway traffic. The key improvement upon the similar construction in FLOVM is that the FLRVM incorporates other car's relative velocity, which can be obtained exactly in ITS environment. However,

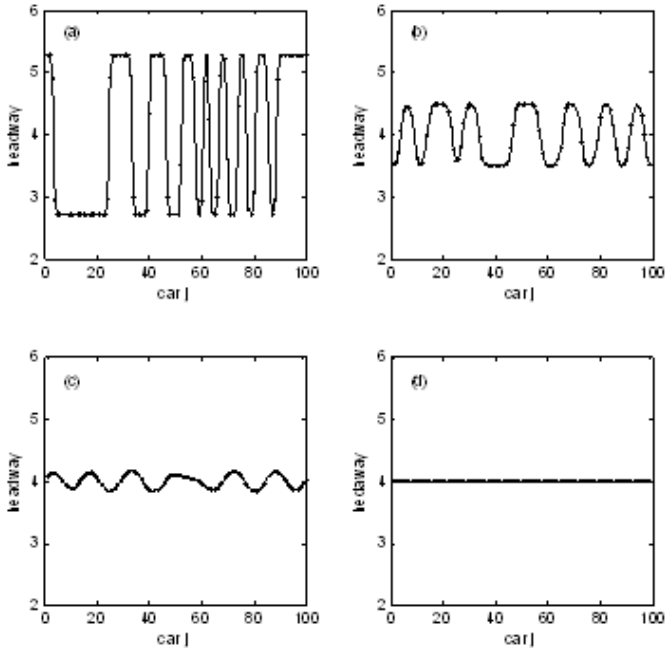

Fig. 2. The snapshots of headway configuration of all cars for (a) $n = 0$,(b) $n = 1$, (c) $n = 2$, and (d) $n = 3$ respectively. ($a = 2$ and $\lambda = 1$).

in the FLOVM, the same extension requires exact other car's position, which is obtained with various errors based on existing skill at present. Then the stability criterion is derived by the linear stability analysis. It has been shown that similar to the FLOVM, the participation of other cars ahead could efficiently suppressed traffic congestion in the FLRVM, which has been verified by direct simulations. In addition, the density wave for traffic flow has been investigated according to the proposed model by the perturbation methods in the stable, unstable and metastable regions. We have found that in the stable traffic region, nonuniform density profile evolves to the uniform density profile by the triangular shock wave, which can be described by the Burgers equation or diffusion equation. We have also found that with an increasing density of traffic flow, the density wave, respectively, is described by the KdV and mKdV equations in the regions of metastability and instability.

This work was supported by the key foundation project of Shanghai (Grant No. 032912066).

References

1. *Traffic and Granular Flow '97*, edited by M. Schreckenberg, D.E. Wolf (Springer, Singapore, 1998)
2. D. Helbing, *Verkehrsdynamik* (Springer, Berlin, 1997)
3. *Traffic and Granular Flow '97*, edited by M. Schreckenberg, D.E. Wolf (Springer, Berlin, 1997)
4. K. Nagel, M. Schreckenberg, J. Phys. I **2**, 2221 (1992)
5. B.S. Kerner, H. Rehborn, Phys. Rev. Lett. **79**, 4030 (1997)
6. B.S. Kerner, H. Rehborn, Phys. Rev. E **53**, R4275 (1996)
7. G.F. Newell, Oper. Res. **9**, 209 (1961)
8. M. Bando, K. Hasebe, A. Nakayama, A. Shibata, Y. Sugiyama, Phys. Rev. E **51**, 1035 (1995)
9. T. Nagatani, K. Nakanishi, Phys. Rev. E **57**, 6415 (1998)
10. T. Nagatani, K. Nakanishi, H. Emmerich, J. Phys. A **31**, 5431 (1998)
11. X. Zhao, Z. Eur. Phys. J. B **47**, 1445 (2005)
12. T. Komatsu, S. Sasa, Phys. Rev. E **52**, 5574 (1995)
13. D. Helbing, B. Tilch, Phys. Rev. E **53**, 133 (1998)
14. R. Jiang, Q. Wu, Z. Zhu, Phys. Rev. E **64**, 017101 (2001)
15. K. Hasebe, A. Nakayama, Y. Sugiyama, Phys. Rev. E **69**, 017103 (2004)
16. K. Hasebe, A. Nakayama, Y. Sugiyama, Phys. Rev. E **68**, 026102 (2003)
17. H.X. Ge, S.Q. Dai, L.Y. Dong, Y. Xue, Phys. Rev. E **70**, 066134 (2004)
18. X. Yu, Chin. Phys. **11**, 1128 (2002)
19. T. Nagatani, Phys. Rev. E **61**, 3564 (2000)
20. M.C. Cross, P.C. Hohenberg, Rev. Mod. Phys. **65**, 851 (1993)
21. S.Q. Dai, Adv. Mech. **12**, 2 (1982) (in Chinese)
22. T. Nagatani, Phys. Rev. E **60**, 6395 (1999)
23. D.A. Kurtz, D.C. Hong, Phys. Rev. E **52**, 218 (1993)
24. H.X. Ge, R.J. Cheng, S.Q. Dai, Phys. A **357**, 466 (2005)